

Effect of Particle Shape on Size Segregation of Particles

Atsuko Shimoska, Iyo Nousou, Yoshiyuki Shirakawa, Jusuke Hidaka

Department of Chemical Engineering and Materials Science, Faculty of Science and Engineering, Doshisha University, 1-3, Tatara Miyakodani, Kyotanabe-shi, Kyoto 610-0321, Japan
ashimosa@mail.doshisha.ac.jp

High-level control of the particle packing structure in a container requires the detailed analysis of particle size segregation during gravity filling. Here, we propose a method for analyzing quantitatively the effect of particle shape on the size segregation of particles using DEM (Distinct Element Method) simulation, which employ spherical particles with an equivalent friction coefficient to efficiently incorporate the effect of particle shape, is proposed.

The simulation of container filling is carried out for particles having a continuous particle size distribution, including different particle shapes. In order to quantitatively evaluate the particle size segregation into the active layer, two metrics are used: a new segregation index indicating the degree of segregation and the percolation index, which evaluates the percolation segregation. Using spherical glass beads, and irregular-shaped Ise sand and alumina particles, the filling behavior of particles into a container are simulated, and the segregation index of those filling layer are estimated. Although increasing the irregularity of particles reduces the mobility of particles, the segregation index of those filling layer conversely become large. Then, the segregation behavior of particles is analyzed using the percolation index. As a result, it is clear that while the coarse particles serve as a frame layer and flow slowly in the center of heap due to the high friction characteristic, the fine particles percolate down; moreover the segregation of coarse particles as a frame layer increase at the bottom of the heap because the velocity gradient of particles under shear flow also increase.

1. Introduction

Particles segregate by their differences in mobility due to the slight differences in the characteristics of the particles, such as the size and shape of each particle, because these particles, which flow while repeatedly colliding with one another, can move freely in the increased void fraction.

As a typical example of segregation, there is the Brazil nut effect, in which coarse particles end up on the surface in the presence of a vibration field; another example is a phenomenon in which a stripe-like separation pattern forms perpendicular to the axis of rotation when a binary mixture of particle sizes is rotated horizontally in a cylindrical drum. These spatial behaviours of particles have attracted interest in many fields, and researchers have worked energetically toward the elucidation of the mechanism behind such behaviour (Henein et al., 1983; Furuuchi et al., 1992).

On the other hand, because particles also segregate gradually under a steady gravity flow, non-uniformity of the components caused by the segregation accompanying the discharge and filling from a container, which is particularly common in many dry powder processes, causes unexpected problems for many products. Therefore, the formation mechanisms and prevention methods of segregation have been investigated experimentally over many years. However, such analysis has almost completely been restricted to surface segregation for ease of observation or modeling of segregation in the underlayer, for which approaches have been developed based on the experimental results of only two or three component systems for ease of analysis (Tüzün and Arteaga, 1992; Shinohara and Golman, 2002; Pudasaini and Mohring, 2002). Moreover, although the influence of particle shape on segregation has been reported by

many (Tang and Puri, 2007; Jha et al., 2008), a quantitative examination of that influence has not been carried out because it is difficult to change only the particle shape in a systematic way in the experiment. In contrast, Distinct Element Method (DEM) simulation is being pursued as a route to obtain the flow behaviour of particles, and has also been an effective method for the analysis of segregation phenomena (Zhu et al., 2009; Li and Yu, 2010). However, the calculation load of the DEM, which solves the equations of motion of each particle directly, is very large, and so it is difficult to treat a system that contains a large number of particles. Additionally, DEM simulations are typically limited to spherical particles from the viewpoint of contact detection. In order to reproduce the shape of a real particle with overlapping spheres, a large number of particles are required, and the limit of the number of particles is to be promoted. Consequently, conditions are also restrained in the simulation because it is difficult to treat particles having irregular shapes and a wide size distribution directly, so quantitative evaluation of the effects of particle shape on the size segregation of particles has not been performed.

To overcome those difficulties, the current authors previously proposed a new DEM simulation that incorporates the effect of particle shape by using the concept of "spherical particles with an equivalent rolling behaviour to the particle with arbitrary shape" (Shimosaka et al., 2010). In the present study, using this simulation method to efficiently incorporate the effect of particle shape on the particle's behaviour, the effects of particle shape on size segregation induced while filling the container are analyzed quantitatively by using the new segregation index.

2. Simulation of container filling

In order to investigate the size segregation induced while filling the container, the simulation of the filling behavior was carried out for particles having a continuous particle size distribution, considering the effects of different particle shapes. In the DEM simulation that considered particle shape using spherical particles, Newton's equations of motion for individual particles are given as Eq.(1)

$$m_i \frac{d\mathbf{v}_i}{dt} = \sum_j (\mathbf{F}_{ij}^n + \mathbf{F}_{ij}^s) - m_i \mathbf{g} \quad I_i \frac{d\boldsymbol{\omega}_i}{dt} = \sum_j (\mathbf{R}_{ij} \times \mathbf{F}_{ij}^s - \mathbf{M}r_{ij}) \quad (1)$$

Here, \mathbf{v} , $\boldsymbol{\omega}$, m and I are the translational velocity, the angular velocity, the mass, and the moment of inertia of a particle, respectively, and \mathbf{R} is the vector from the center of a particle to the particle surface. Also, \mathbf{F}_{ij}^n and \mathbf{F}_{ij}^s are the normal and tangential force actors arising due to inter-particle contact.

Additionally, we defined the dynamic friction moment $\mathbf{M}r$ as Eq. (2)

$$\mathbf{M}r_{ij} = \mu_{\text{rol}}(\alpha, \boldsymbol{\omega}) R_i \mathbf{F}_{ij}^n \hat{\boldsymbol{\omega}} \quad (2)$$

Here, the coefficient of rolling friction $\mu_{\text{rol}}(\alpha, \boldsymbol{\omega}) = \alpha \omega_{ij}^2$ was introduced as a function of the coefficient α , which is related to the particle shape, and the component of the relative angular velocity vector $\boldsymbol{\omega}$ where the relative sliding velocity component has been eliminated. Also, $\hat{\boldsymbol{\omega}}$ is the normalized vector $\boldsymbol{\omega}_i / |\boldsymbol{\omega}_i|$.

The photographs of the types of particles used in the simulation and the α coefficients related to the shapes of the particles are shown in Figure 1. These values of α were determined from the Fourier coefficients obtained from the Fourier transform of the particle contours and the coefficient of rolling friction obtained from the polygonal pillar-rolling experiments. Larger values of α indicate a more irregular shape and a higher rolling resistance. These coefficient values, the reliability of the proposed shape descriptions of irregular particles, and their equivalent rolling friction coefficient were all confirmed by the comparison of the simulated flow behaviours on the inclined plate with the experimental ones in the previous paper (Shimosaka *et al.*, 2010). Other simulation conditions are listed in Table 1. Although the particles used were spherical glass beads, irregularly shaped Ise sand, and alumina particles, all of the values of the glass bead except the friction coefficient were used in modeling all three types of particles, so that we could investigate only the effect of particle shape on size segregation. First, the log-normal number

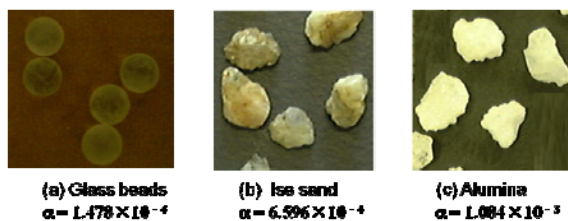


Figure 1: Photographs of different particle types and corresponding coefficients

size distribution of 100,000 particles in the size range of 2–20 mm, with a geometric mean size of 8.4 mm and a geometric standard deviation of 1.38, was generated. The particles were arranged randomly with a 38% packing fraction within the feed chute (H12.00 × W0.03 × D0.10m), which was set at the upper left side of the square-shaped container (H0.50 × W0.75 × D0.10m). Then, the particles within the feed chute were released and fell down at a uniform velocity of 0.5 m/s, filling the

Table 1: Mechanical properties and physical constants

		Acryl	Glass bead	Ise sand	Alumina
Density	[kg/m ³]	1180	2650	2650	2650
Young's modulus	[Pa]	2.94 × 10 ⁹	4.90 × 10 ⁹	4.90 × 10 ⁹	4.90 × 10 ⁹
Poisson's ratio	[-]	0.300	0.230	0.230	0.230
Coefficient of repulsion					
(particles)	[-]		0.0799	0.0799	0.0799
(particle-acryl wall)	[-]		0.182	0.182	0.182
Coefficient of sliding friction					
(particles)	[-]		0.130	0.351	0.441
(particle-acryl wall)	[-]		0.396	0.618	0.689

First, the particles in the size range 2 – 20mm were divided into 5 components (Dp1 - Dp5) in size intervals of 4 mm, and the number concentration distributions $C_i(x,z)\%$ in the particle filling layer which is dynamic state variable, was calculated. Here, the particle filling layer was divided into one section along the y-axis, nine sections along the x-axis, and eight sections along the z-axis. To indicate the degree of segregation within the layer, the segregation index I_{seg} is defined as Eq.(3)

$$I_{seg}(i) = \frac{1}{x_{max}} \sum_{x=1}^{x_{max}} \left| \sum_{z=1}^{z_{max}} C_i(x, z) / z_{max} - 100 / x_{max} \right| \quad (3)$$

Here, z_{max} is the number of divisions from the bottom to the surface in the direction of the z-axis and x_{max} is the number of divisions (9) along the x-axis. This index evaluates how much the average concentration of each size component in the z-direction, $\sum_{z=1}^{z_{max}} C_i(x, z) / z_{max}$, is segregated over the x-direction. For example,

when the average concentration in the z-direction is 11% for all values of x, the segregation index indicates that there is no segregation since $I_{seg} = 0$. Furthermore, to evaluate the percolation process into the active layer, which is an important segregation mechanism, the percolation index a_{ij} is defined by applying the screening model (Miwa 1981) as Eq. (4).

$$\log \left(\frac{\sum_{z=1}^{z_{max}} C_i(x_{n+i}, z) / z_{max}}{\sum_{z=1}^{z_{max}} C_j(x_{n+i}, z) / z_{max}} \right) = \log \left(\frac{\sum_{z=1}^{z_{max}} C_i(x_n, z) / z_{max}}{\sum_{z=1}^{z_{max}} C_j(x_n, z) / z_{max}} \right) - a_{ij} (x_{n+i} - x_n) \quad (4)$$

The slope of the straight line obtained by plotting the logarithm of the ratio of the average concentration in the z-direction of large j particles to small i particles between two points on the flow direction x_n and x_{n+i} is a_{ij} . This indicates the ease with which percolation screens the small i particles with the gap between large j particles. When the ratio of the average concentration of large j particles to small i particles between points became 1/10 by the percolation of i particles, the percolation index is set to $a_{ij}=1.0$, and it is set to $a_{ij}=0.0$ when percolation does not arise.

4. Effect of particle shape on size segregation

Figure 2 shows snapshots of the container depicting the filling behavior and the velocity vectors of particles in the example of Ise sand. Here, particle color represents particle size, and the yellow color indicates coarser particles. The particles flow in the shear layer and the finer particles are gradually percolated with the coarser ones, resulting in them settling on the stationary under layer, as shown by the velocity vectors of the particles. As a result, the finer particles were segregated at the position below the chute, and the coarse particles were segregated at the ending point of the flow.

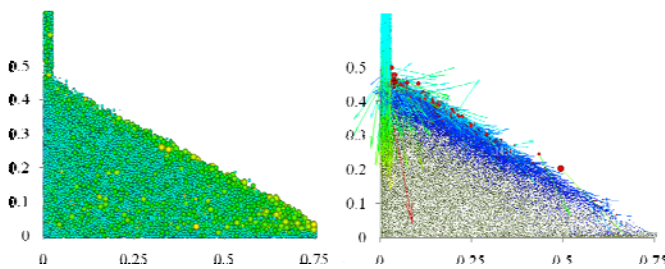


Figure 2: Filling behaviour and velocity vectors of particles in the container (Ise sand)

container from the opening in the lower part of the chute under gravity field.

3. Methods of evaluation for size segregation

In order to evaluate the particle size segregation that occurs during gravity filling of the container, the new segregation index I_{seg} and the percolation index a are defined.

In order to visualize the degree of these segregations, distribution maps for the sedimentary layer for each particle size range were generated and are shown in Figure 3. This figure confirms that the finer particles of size 2 – 8 mm segregate on the left side below the chute. The particles of size 8 – 12 mm flow gradually to disperse over the whole container, and then the segregation of the particles of 12 – 16 mm size pushes them preferentially to the ending point of the flow, on the right

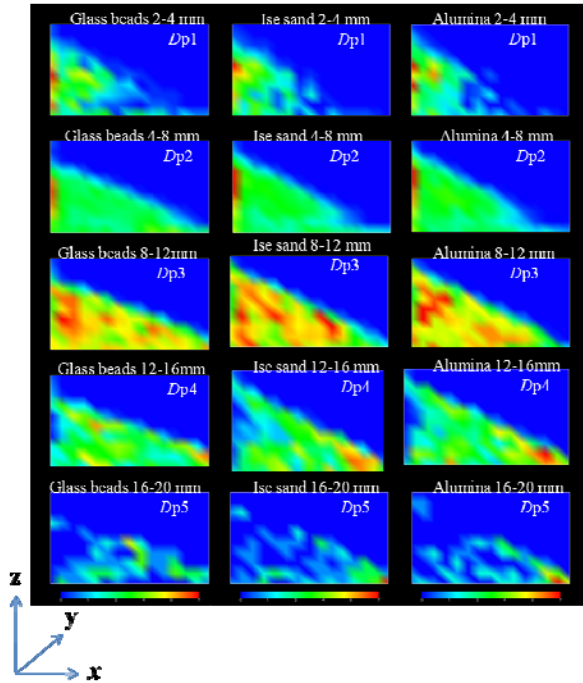


Figure 3 : Maps of the number of particles in each size range

side of the container. This tendency becomes still more remarkable in the distribution of particles of size 16 – 20 mm, and there are many coarse particles at the ending point of the flow as they are more irregularly shaped particles.

Then, in order to evaluate the size segregation quantitatively, the average concentration of each size component in the z-direction, was calculated over the x-direction according to the definition in Section 2. It was found that the smallest component of D_{p1} acquired a significant non-uniform spatial distribution due to the segregation process. The average concentration profiles of D_{p1} and of the largest component of D_{p5} , for the cases of glass beads, Ise sands, and alumina particles were plotted to investigate the effect of particle shape on the horizontal distribution of particle concentration, as shown in Figure 4. In this figure, position 1 is on the left end of the container below the chute, and position 9 is on the right end. Also, the dashed line shows an average concentration value of 11%, which indicates the absence of segregation. This figure indicates that the gradient of the particle concentration is large and that the size segregation increases as the particles becomes more irregular in shape. In the

largest component of D_{p5} for which the segregation effect was especially weak for the glass beads, the segregation at the terminal point of the flow is very large in the case of Ise sand or alumina particles. Then, values for the segregation index I_{seg} , indicating the degree of segregation within the layer, were calculated using Eq. (5), as shown in Figure 5. There is little difference in the index between the middle components of D_{p3} and D_{p4} , but the effect of particle shape on the indexes is confirmed in the cases of the smallest component of D_{p1} and the largest component of D_{p5} .

In the past, there have been many attempts at modeling by treating either the different mobility values of trajectories or the different rolling behaviors of particle (both caused by the particle properties, such as size, density, and shape), as the basic segregation mechanism in flowing particles. Similarly, percolation segregation, in which finer particles move down through the gaps between coarse particles to be in a flowing layer, has received considerable study. According to these segregation mechanisms, it is predicted that segregation becomes noticeable when the particles have a wider size distribution, a lower feeding rate, and higher flowability because the differences in mobility of individual particles are amplified. However, increasing the irregularity of the particles reduced the mobility of the particles; nevertheless, the

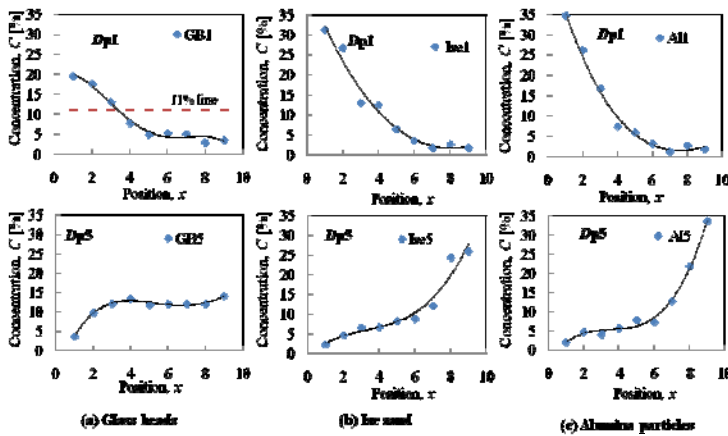


Figure 4 : Effect of particle shape on horizontal distribution of particle concentration (D_{p1} , D_{p5})

segregation index values obtained by changing only the particle shape conversely became large.

Then, the effect of particle shape on the size segregation was investigated in detail by analyzing the relationship between the percolation index a_{ij} and the particle size ratio. Figure 6 shows the relation between the horizontal position x_n and the logarithm of the ratio of the average concentration of finer particles (those in component D_{p1} and D_{p2}) for each particle shape. The linear correlation, which gives the percolation index, is found in the position range from 2 to 7. The

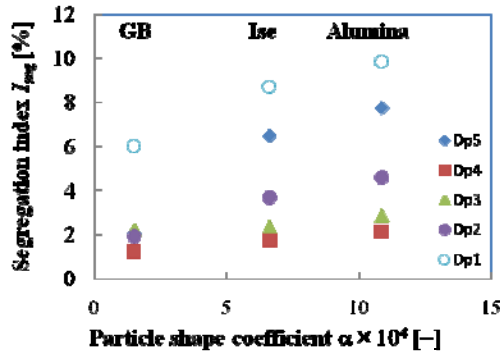


Figure 5 : Effect of particle shape on segregation index of multi-sized particle

percolation of the irregularly shaped particles progresses gradually at the left side (positions 1–7), and conversely it becomes intense at the right side (positions 7–9).

Then, the percolation index of the left side was set to a^1 , and that of the right side was set to a^2 ; the percolation index of each particle shape between the two components is shown in Figure 8. As for a^1 , $a^1_{2,3}$ of the middle components is very small as predicted; in contrast, $a^1_{1,2}$ of the finer components is large. Also, the particle shape has little effect on these indexes, but, $a^1_{1,5}$ which is the index of Dp1 to Dp5, becomes extremely large for the irregular particles. Thus, the percolation segregation of the smallest particles at the position below the chute can be seen to be intense for the irregularly shaped particles. As for a^2 , the index of the glass beads is almost 0; by contrast, that of the irregularly shaped particles is very large, and the largest differences are in $a^2_{4,5}$ between the glass beads and the other two types of particles. This figure shows that the segregation of the coarse particles is accelerated at the end of the flow, along

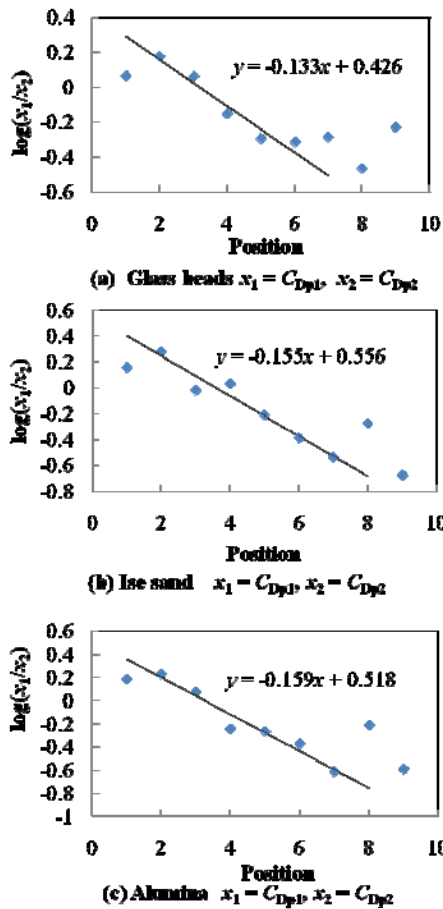


Figure 6 : Percolation index of fine particles

figure clearly indicates that the segregation of the finer particles at the left position below the chute, as shown in Figure 6, was caused by the percolation. Moreover, the percolation index increases as the shape irregularity increases, although the difference in the shape was not clear in Figure 6. Additionally, the results for the coarse particles (Dp4 and Dp5) are shown in Figure 7. In two of the correlations, the slope differs between the left and right sides, and the tendency of both indexes changes greatly with the shape of the particles. That is, it is found that the percolation of the spherical particles arises at the left side (in positions 1–3), but it does not progress to the right side (positions 3–9) to the end point of the flow, because $a_{4,5}$ is very small. By contrast, the

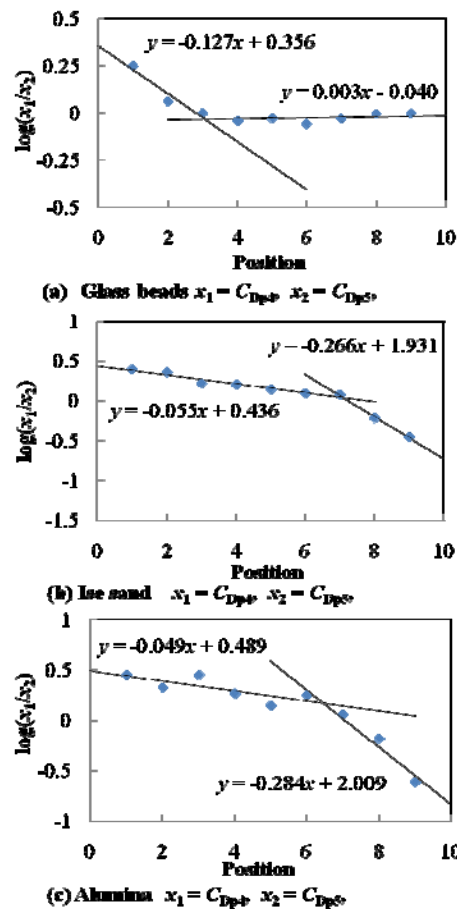


Figure 7 : Percolation index of large particles

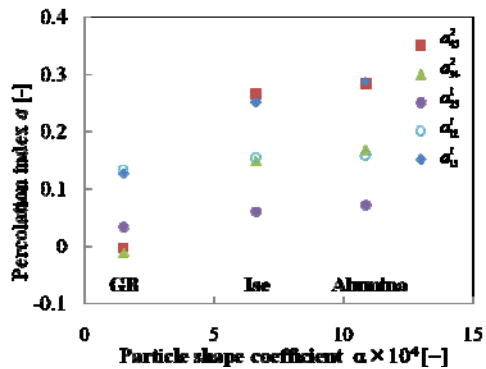


Figure 8 : Effect of particle shape on percolation index

with the free flight and rolling on the surface of the heap. These results suggest that, in the case of irregularly shaped particles with a high friction characteristic, while the coarse particles serve as a frame layer and flow slowly in the center of the heap, the fine particles percolate down; moreover, the segregation of the coarse particles as a frame layer increases at the bottom of the heap, because the angle of repose formed during the filling is large, and the velocity gradient of the particles under the shear flow also increases.

4. Conclusions

The effects of particle shape and size distribution on the size segregation of particles occurring during gravity filling of a container have been analyzed quantitatively by using DEM simulation, employing spherical particles with an equivalent friction coefficient to efficiently incorporate the effect of particle shape. Two metrics have been defined: the segregation index I_{seg} , which uses the number concentration distribution $C_i(x,z)\%$ in the particle filling layer in order to indicate the degree of segregation into the active layer, and the percolation index a_{ij} , which evaluates the percolation segregation by applying the screening model.

Using the equivalent friction coefficients of spherical glass beads, irregularly shaped Ise sand, and alumina particles, the filling behavior of particles with a size distribution having a geometric standard deviation of 1.38 was simulated. The segregation indexes for those filling layers were estimated, and so the effect of particle shape on the indexes was confirmed in the case of the smallest component of D_{p1} and the largest component of D_{p5} . Conversely, the index values became large, although increasing the irregularity of the particles reduced the mobility of the particles. Then, the segregation behavior of the irregularly shaped particles was analyzed using the percolation index. As a result, it is clear that while the coarse particles serve as a frame layer and flow slowly in the center of the heap due to the high friction characteristic, the finer particles percolated down; moreover, the segregation of coarse particles as a frame layer increased at the bottom of the heap because the velocity gradient of particles under shear flow also increased. Thus, because the proposed method could accurately estimate the effect of particle characteristics on size segregation, we expect that this method will be applied to the design of particle characteristics, which reduce the size segregation in filling processes.

References

- Jha A. K., Gill J. S., Puri V. M., 2008, Percolation Segregation in Binary Size Mixtures of Spherical and Angular-Shaped Particles of Different Densities, Part. Sci. Technol., 26, 482-493.
- Knight J. B., Jaeger H. M., Nagel S. R., 1993, Vibration-induced size separation in granular media: The convection connection, Phys. Rev. Lett. 70, 3728-3731.
- Li J., Yu A. b., 2010, Spontaneous Inter-Particle Percolation: A Kinematic Simulation Study, Powder Technol., 203, 397-403.
- Miwa S., 1981, Introduction of Powder Technology, pp.126-127, Nikkan Kogyo Shinbun, (in Japanese).
- Pudasaini S. P., Mohring J., 2002, Mathematical Model and Experimental Validation of Free Surface Size Segregation for Polydisperse Granular Materials, Granular Matter, 4, 45-56.
- Rapaport D. C., 2007, Radial and axial segregation of granular matter in a rotating cylinder: A simulation study, Physical Review E 75, 031301-1-11.
- Shimosaka A, Akashi M., Matsumoto H., Shirakawa Y., J. Hidaka, 2010, DEM Simulation for Irregular Particles using the Equivalent Rolling Friction Coefficient, Kagaku Kogaku Ronbunshu, 36, 86-93.
- Shinohara K., Golman B., 2002, Particle Segregation of Binary Mixture in a Moving Bed by Penetration Model, Chem. Eng. Sci. 57, 277-285.
- Tang, P., Puri V. M., 2007, Segregation Quantification of Two Component Particulate Mixtures—Effect of Particle Size, Density, Shape, and Surface Texture, Part. Sci. Technol., 25, 571-588.
- Tüzün U., Arteaga P., 1992, A Microstructural Model of Flowing Ternary Mixtures of Equal-density Granules in Hoppers, Chem. Eng. Sci., 47, 1619-1634.
- Zhu H. P., Rahman M., Yu A. B. 2009, Numerical investigation of particle percolation in a packed bed, Miner. Eng., 22, 961-969.